Research Repository UCD

Title	Using Terrestrial Laser Scanning for Dynamic Bridge Deflection Measurement
Authors(s)	Truong-Hong, Linh, Laefer, Debra F.
Publication date	2014-08-13
Publication information	Truong-Hong, Linh, and Debra F. Laefer. "Using Terrestrial Laser Scanning for Dynamic Bridge Deflection Measurement," August 13, 2014.
Conference details	IABSE Istanbul Bridge Conference, Istanbul, Turkey, 11 - 13 August 2014
Item record/more information	http://hdl.handle.net/10197/7495

Downloaded 2026-05-21 17:15:19

The UCD community has made this article openly available. Please share how this access benefits you. Your story matters! (@ucd_oa)

© Some rights reserved. For more information

Using Terrestrial Laser Scanning for Dynamic Bridge Deflection Measurement

Linh Truong-Hong[1] and Debra F. Laefer[2]

ABSTRACT

Heavy vehicular traffic and aggressive environmental conditions can cause unexpected bridge deterioration, thus requiring periodic inspections to identify and assess possible defects. One indicator is the amount of vertical deflection that occurs during loading. Monitoring vertical bridge deflection through traditional surveying typically requires multiple instruments and extensive time in the field, along with their affiliated costs. A terrestrial laser scanner (TLS) can generate a million data points per second with millimeter level accuracy, thus offering the possibility of changing how vertical deflections of bridge girders are checked. This paper presents a preliminary investigation into using TLS to collecting vertical bridge displacements during dynamic loading. In this work, a point-surface based method is proposed to calculate the difference in elevation of a bridge girder at unloaded and loaded conditions. The technique is applied to the Loughbrickland Bridge in Northern Ireland.

Keywords: Terrestrial laser scanning; point cloud; bridge inspection; dynamic deflection

Introduction

A bridge's performance life can be reduced unintentionally by excessive loading and environmental impacts. To counter this, knowledge of a bridge's performance level is needed to schedule to timely and sufficient maintenance, which helps to prevent catastrophic damage, particularly for aging bridges. For periodic bridge assessment, many types of instruments have been developed and applied. These include strain gauges, fiber optic sensors, and displacement transducers [1]. Despite their very high accuracy, these instruments are expensive, discrete in their measurements, and must be attached to the structure. Noncontact measurement techniques such as photogrammetry have also been tried for both deformation and displacement measurement [2, 3]. While the accuracy of photogrammetry can be at the millimeter level, the method has its own drawbacks including the following: (i) requires multiple cameras, (ii) needs the exact distance from each camera to the structure to be known, and (iii) necessitates a fixed reference point [4].

The current generation of terrestrial laser scanners (TLS) has capability of rapidly acquiring high data density at millimeter accuracy without contacting the structure that is to be documented and does not have the known limitations of photogrammetry. TLS has been established in various related civil engineering applications including biological crust monitoring [5], building inspection [6], and structural analysis [7]. For bridges the work has to date been limited largely to deflection or clearance measurement under static loads [8, 9]. This paper proposes a new procedure for using TLS to collect bridge deflection data under dynamic loading.

Background

The first published attempt at capturing vertical deflections of a bridge with TLS was done by Lichti et al. [10] in 2002 on a Wooden bridge on the Toodyay-Goomalling road, in Perth, Western Australia that was subjected to 95 different static load condition ups to 65.75 tons. The stringer's cross-section from the point cloud was reconstructed by second-order least squares. Subsequently, vertical stringer displacements were estimated by comparing fitting

[1] Research scientist, Urban Modelling Group (UMG), School of Civil, Structural and Environmental Engineering (CSEE), University College Dublin (UCD), Dublin 4, Ireland. Email: *linh.truonghong@ucd.ie*

[2] Associate Professor, Head UMG, CSEE, UCD, Dublin 4, Ireland. Email: *debra.laefer@ucd.ie*, *corresponding author*

lines of the bottom and top fibers under loaded and unloaded conditions. The stringer deflections derived from the TLS were larger than those obtained from digital images, where the root mean square errors (RMSE) were ±9.1mm and ±4.9mm for the bottom and top fibers of the stringer, respectively.

Subsequently, Zogg and Ingensand [11] used TLS to monitor deformations of the Felsenau viaduct bridge when subjected to a static load of 54 tons. The test was performed at several sections of the viaduct. The Geomagic Qualify program was used to extract the vertical displacements by comparing 3D point clouds under the loaded and unloaded conditions. The TLS-based results differed from precise levelling based ones by less than 3.5mm, with a mean residual less than 1.0 mm. Similar work by Lovas et al. [12] reported TLS-based displacements as larger than ones from precise levelling but less than those from a total station approach. Similarly, in capacity testing by the Florida Department of Transportation (FDOT) of the I10-exit 30 bridge in Tallahassee, Florida, TLS was used to record deflections under static loads up to 87.1 tons [13]. The TLS based results differed no more 2 mm from traditional surveying results and required only 5% of the time.

TLS is also being used to determine minimum vertical clearance to prevent vehicular collision. Kretschmer et al. [14] did this for the bridge at highway No. 5 at the Freiburg center exit in Germany. Vertical displacement was determined as the distance between the section at a specific point on the road (assumed as the plane) and a projection of this section onto the bottom beam of the bridge. The TLS results differed by as much as 3cm compared to ones based on conventional measurements. In a different approach, Riveiro et al. [9] used a 3D curve-fitting of a pavement surface and a beam camber from TLS data points to calculate a vertical clearance. An underpass bridge on the AP-9 in the Northwest region of the Iberian Peninsula, in Spain was used to compare TLS- and photogrammetric-based techniques. The TLS- and photogrammetric-based data generated respectively a minimum vertical clearance 9mm and 11mm larger than those from total station measurements. In a related approach based on TLS scan data, Liu et al. [15] proposed a point-based method to determine the vertical bridge clearance, where the difference of z-coordinates in the point clouds of the ground and the bridge deck was compared along the same vertical scan line. In a study of 4 bridges in North Carolina, the maximum difference of vertical clearance based on TLS versus the reported inventory was 0.23m. The minimum was 0.00m.

Equipment

A current TLS unit can collect over million points per second through either triangulation or ranging [16]. The ranging scanners measure the distance between the transmitter and reflecting surface based on the travel time between the signal transmission and reception. This is called time of flight (ToF) of a laser pulse [17]. This type of scanner is often used for measurements of large structures. In this paper, a ToF scanner was used.

The scanner provides the scanned points by a series of range measurements, where scanned point patterns are collected in a uniform, angular distribution in both horizontal and vertical planes. This is controlled by rotating and nodding mirrors and rotating head mechanisms [18]. As such, each sampled point is defined by spherical coordinates with the range measurement, R, horizontal direction, θ, and vertical angle, φ (Fig. 1). The raw scanned point (R, θ, φ) is automatically converted into three-dimensional (3D) Cartesian coordinates (x, y, z) by the scanner software, where the origin coordinate is taken to be at the scanner.

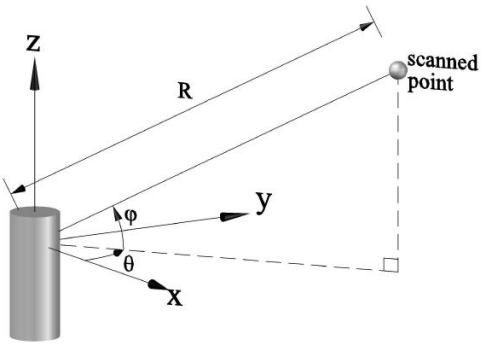

Fig. 1. The principal of laser beam scanning

A range measurement is defined as the distance from the transmitter to the reflecting surface, R, as expressed in Eq. 1:

$$\mathbf{R} = \frac{1}{2}\mathbf{ct} \tag{1}$$

where t is the time interval between the emission and the pulse and its reception of the backscattered portion, and c is the velocity of light in air ($3x10^8$ m/s). The scanner accuracy is based on the accuracy of the time measurement of the electronics integrated into the circuit, (Eq. 2). Furthermore, the ranging accuracy is inversely proportional to the signal to noise ratio, which depends on various factors such as the power of the received signal, input bandwidth, background radiation, and amplifier noise [17, 19].

$$\Delta\mathbf{R} = \frac{1}{2}\mathbf{c}\Delta\mathbf{t} \tag{2}$$

In addition to the 3D coordinates of the scanned points, output data from the scanner also includes intensity values and photographic red, green and blue (RGB) values.

Table 1 provides abbreviated technical specifications for a sampling of popular scanners Pulse systems are suited for long-range scanning (up to 6000m). The beam diameter is the diameter along any specified line that is perpendicular to the beam axis and intersects it. This parameter can cause positional uncertainty [20], where the point accuracy can be less than 2mm. Moreover, the scan angle step, which is the ability to resolve two equally intense point sources on adjacent sight lines, is a function of the spatial sampling interval and the laser beam diameter. To obtain a sufficient sampling step for estimating the level of detail from TLS data, Lichti and Jamtsho [20] suggested that the sampling interval be set equal to the beam width. The minimum incremental angle reported by the Leica scanner is 0.00008˚ corresponding to the minimum sampling step of 0.8mm at the range of 10m [21]. In TLS, a rotating optical device is used in transmitting the laser beam to an object and receiving the return beam; the two angles are theoretically the same. The accuracy angle is used to measure the difference between the two angles through a mechanical axis or other optical rotating device. For the units presented in Table 1, the largest angular error is 0.046˚. Finally, the current generation of scanners offers a wide-angle scanning range in both the horizontal and vertical directions, as well as incredibly fast acquisition rates [21, 22].

Table 1. Summary of technical specifications of commercial scanning system

Brand	**Optech Incorporated** [23]	**RIEGL Laser** [24]	**Leica Geosystems** [21]	**Trimble** [22]
System	ILRIS-HD	RIEGL VZ-6000	Leica ScanStation P20	TX8
Metrology Method	Pulse	Pulse	Pulse	Pulse
Min. / max. range (m)	3.0 / 1200	5 / 6000	0.4 / 120	0.6 / 120
Point accuracy	3-4mm @ 100m	15mm @ 150m	3mm @ 50m	< 2mm
Beam diameter	19mm @ 100m	15mm @ exit; 60mm @ 500m	2.8mm at front window	6-10-34mm @ 10-30-100m
Scan angle step size H/V (^{0})	0.000745	0.002-3/ 0.002-0.280	0.8mm@10m: Minimum point spacing	0.005
Scan angle accuracy H/V (^{0})	0.046	0.0005	0.002	0.005
Field of view H/V (^{0})	40/40	360/60	360/270	360/317
Acquisition rate (KHz)	10	300	1000	1000

Measurement deformation model

Notably, the technology only acquires a 3D set of discrete points. Thus, a surface is scanned instead of a specific point or line. To compute bridge displacements during a dynamic event using TLS data, the proposed method assumes the following: (1) across the relatively small investigated area, deflection differences are minor; (2) the time-lapse due to the mirror rotating in order to take an adjacent vertical scan line is ignored, as this is very small compared to the scanning time of one vertical profile; (3) the scanning time for collecting each data point in the same scan line is equal. The first assumption allows bridge deflections derived from the scanned area to be consider as the deflection of the cross-section of interest. The deflection is determined based on the relative position of the point cloud of the selected area under the loaded and unloaded conditions. The other two assumptions are used to determine the scanning time of each data point.

Fixed ground 3D TLS scan is taken of a predefined, surface containing the cross-section of interest (Fig. 2a). During scanning process, one mirror rotates about the horizontal axis to generate a vertical profile, while another mirror rotates about the vertical axis in a clockwise direction to generate an adjacent vertical profile. The vertical and horizontal sampling intervals are controlled by the scan angle steps in the vertical and horizontal directions (Table 1). The scan patch is rectangular and is comprised of N scan lines, with M points in each scan line (Fig. 2a). As each scanned point (represented by an x, y, and z coordinate) is part of the topology of the object's surface, theoretically the scanned point can be tracked as the object moves. Fig. 2b shows the elevation of the bottom beam's fiber when loaded and unloaded.

The absolute vertical displacements during dynamic loading are determined by comparing point clouds of the surface captured under loaded and unloaded conditions. This requires two main steps: (i) calculation of the vertical offset of the relevant points by using a point-surface based method and (ii) determination of the time at which each data point was captured. The workflow is shown in Fig. 3. In this study, the point cloud from the unloaded condition is considered as the reference data set (a set of $\mathbf{P}_r = \{p_{r1}, i = \{1,..., n_r\}\}$ in $\in R^3$) and that from the loaded condition as the sample data set (a set of $\mathbf{P}_s = \{p_{s1}, i = \{1,..., m_s\}\}$ in $\in R^3$) (Fig. 3).

Firstly, for each given point (p_{si}) in the sample data set, its neighboring points ($\mathbf{q} = \{q_{rj}, j = \{1,\ldots,k\}$ from the reference data are extracted. These are the points closest to the given point in Euclidian space. In this study, 16 neighboring points were empirically chosen. This step extracts the point representing the local surface, *S*, of the object before deflection. Secondly, *S* is fitted from the neighboring points, **q,** by using a least squares method. The scanned data

may contain noise, which affects the quality of the fitting surface. To minimize this effect, any point having a large residual (that is a distance from this point to the fitting surface) is removed from the neighboring points, where the maximum noise level of the scanner is considered as the residual threshold. The local surface is iteratively fitted based on remaining points, until there is no residual exceeding the noise threshold. Finally, the distance $d(p_{si}, p'_{si})$ as the vertical displacement is computed, where the point p'_{si} is the intersection between a ray though p_{si} with a direction vector [0, 0, 1] and the fitting surface (S) (Fig. 3).

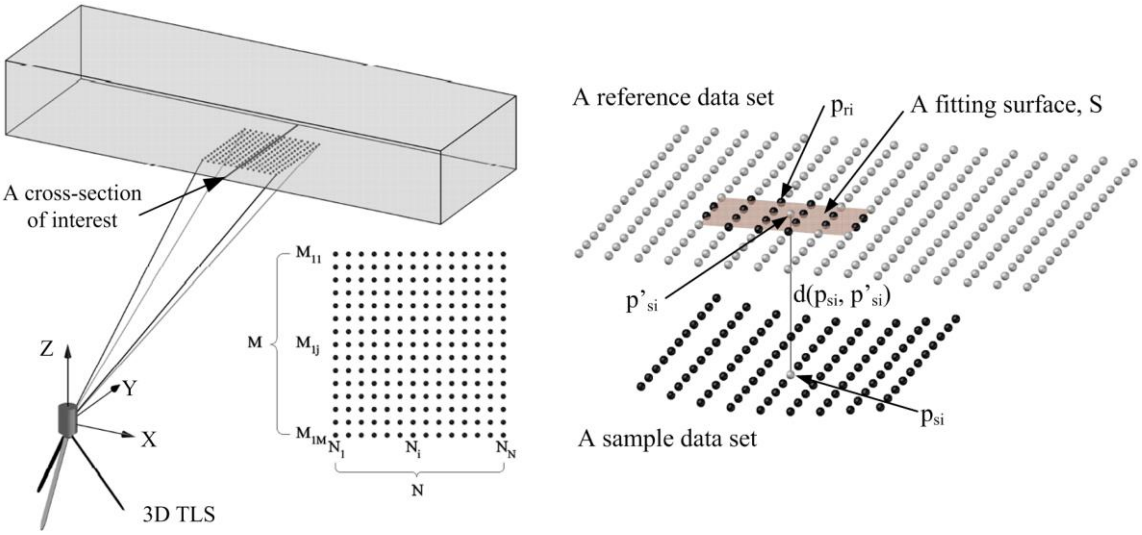

a) Scan pattern common for 3D TLS

b) Point-Surface based method for deflection measurement

Fig. 2. Deflection measurement of the bridge based 3D TLS point cloud

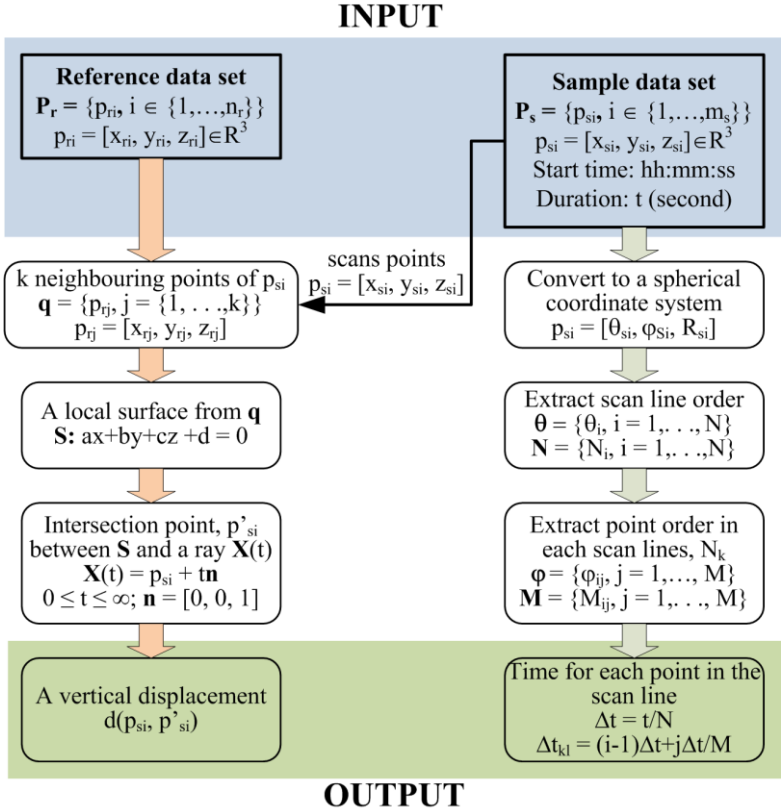

Fig. 3. Workflow of defined scan time for each point in the sample data

In stage two, the scanning time of each data point in the sample data set is determined from time information collected by the scanner. Based on the equipment's scanning mechanism, the data points on the scan lines have the same azimuth angle, θ, and the point order in the scan line is based on the polar angle, φ, where the data points are described in a spherical coordinate system. Firstly, the point cloud in the sample data set is converted to the spherical coordinate system, which is described as $p_{si} = [\theta_{si}, \varphi_{si}, R_{si}]$, where θ_{si} and φ_{si} are, respectively the azimuth and polar angles, and R_{si} is the distance from the origin to a point. Points having the same value as the azimuth angle, θ_{si} are assigned the same scan line number, where the scan line with the maximum azimuth angle is the first scan line. Notably, as the points of the same scan line often do not belong to the same azimuth angle, the tolerance angle, Δθ was added to extract these points. In this context, a point is assigned to the scan line N_i, if its azimuth angle is within $(\theta_i - \Delta\theta)$ to $(\theta_i + \Delta\theta)$, where θ_i is the azimuth angle of the scan line N_i. Using a tolerance angle Δθ of $1/10^{th}$ of the horizontal angle step was observed to be successful in extracting the scan lines. Secondly, the point order in each scan line, N_i is subsequently determined based on the polar angle φ_{ij}, where the first point order has the smallest polar angle in the scan line. Finally, the scanning time for each scan line and for point j in the scan line i are determined with Eq. 3 and 4, respectively.

$$\Delta t = \frac{t}{N} \tag{3}$$

$$\Delta t_{ij} = (i-1)\Delta t + j\frac{\Delta t}{M} \tag{4}$$

where t is a duration for completing a scan of the selected object, N is the total number of the scan lines, and M is the total points of the scan line N_i (Fig. 2).

Through the coordinates and the scanning time of each data point, the vertical displacements at the specific location of the bridge are determined by the procedure above. As data noise still influences vertical displacement calculation, smoothing vertical displacements through the application of an average displacement over the time step is done, as given in Eq. 5:

$$\Delta d_{t_i} = \frac{1}{m}\sum_{j=t_i-\Delta t/2}^{t_i+\Delta t/2} d_{t_j} \tag{5}$$

where d_{ti} is the vertical displacement at time t_i, m is the number of displacements recorded from the period, $t_i - \Delta t/2$ to $t_i + \Delta t/2$, Δt is the time step and d_{tj} is the displacement at time t_j in the period, $t_i \pm \Delta t/2$.

Experimental tests & results

Measurement bridge description

Monitoring vertical displacement of a bridge was performed on the underpass of the Loughbrickland Bridge on Highway A1 connecting between Belfast and Newry, in Northern Ireland. The bridge is an integral abutment bridge consisting of 29 beams, 20.18m long, 36.29m wide, with a 69-degree skew. It has three traffic and pedestrian lanes in each direction (Fig. 4a&b). As freight vehicles operate in lane 1, the middle cross-section of the beam No. 8 was selected to monitor the vertical deflection (Fig. 4c). The test was conducted with a Leica P20 TLS unit whose technical specifications are shown in Table 1.

In this work, the selected area was approximately 30mm wide by 30mm long (Fig. 4c). The selected area was scanned with an angle spacing of 0.0045 degree from a distance approximate 7.5m. The expectation was to obtain a sampling step on the scanned area every

0.6mm (theoretically generating 2705 points over the 30mmx30mm area). This was largely confirmed with a total of 2625 points being collected per each scan. The scanning time for a scan is approximate 11 second. As such, to monitor the dynamic deflection of the bridge girder, multiple scans were set up to scan the selected area over period. Notably, an elapsed time between two consecutive scans is 6 seconds. The reference data set was collected when the bridge was unloaded.

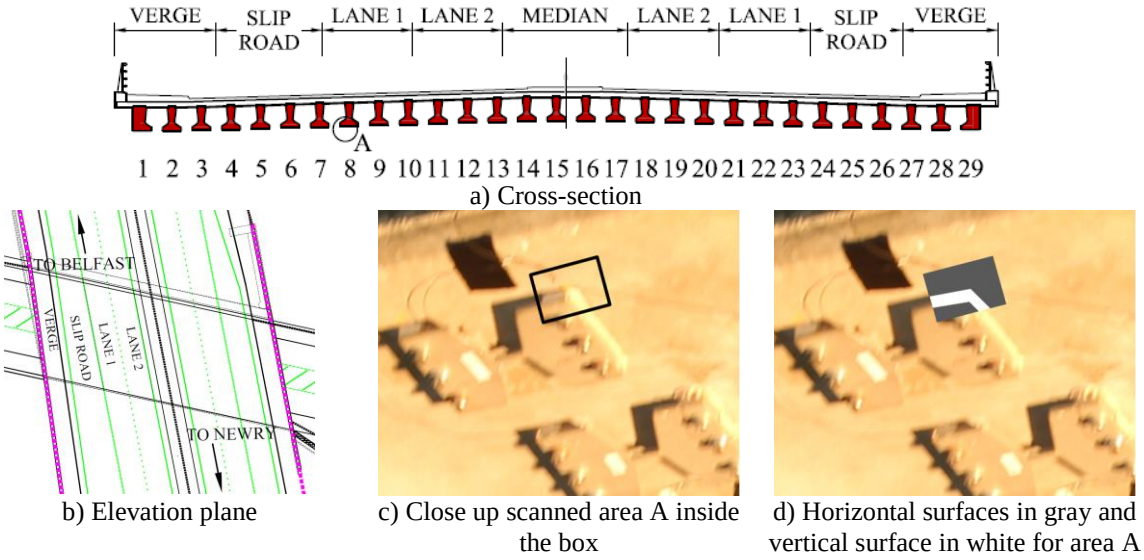

a) Cross-section

b) Elevation plane

c) Close up scanned area A inside the box

d) Horizontal surfaces in gray and vertical surface in white for area A

Fig. 4. Configuration of Loughbrickland Bridge

Results

The proposed method was implemented in a Matlab script [25]. The input data were reference and sample point cloud data sets, including the starting time and collection duration for each data set. Examples are shown in Fig.s 5a-b. Only data from the horizontal surfaces of the beam and steel plate (gray color in Fig. 4d) are used to compute vertical displacements of the beam, as the vertical surfaces of the steel plate (white color in Fig. 4d) do not change. Notably, co-registration of the various scans is unneeded as all data sets are collected from the same scan station.

In this work, a filtering process is implemented to classify points in the scan line as belonging to either the horizontal plane or the vertical one. A given point is considered to be on the vertical plane, if a difference in elevation between this point and its adjacent point in the same scan line is larger than a distance between them on the horizontal plane; otherwise, this point is on horizontal plane. Results of the filtering process are illustrated on Fig. 5d-f.

Subsequently, from each remaining point in the sample data set, a vertical displacement is computed as part of the workflow in Fig. 3. However, the original sample data set is used to calculate scanning time for each point, which is based on a total of points, input start time and scanning duration of the sample data set. Then, the scanning time of the remaining points in the sample data set is retrieved. The direct results are shown in Fig. 6a and those after applying the smoothing (Eq. 5) are shown in Fig 6b, where a time step by 0.125s is used. Displacements directly derived from data points in the sample data set mostly vary ± 1mm. After smoothing, the displacements were in a tighter range of ± 0.5mm. Fig. 7 shows the vertical and smoothed displacements from four consecutive scans. Notably, as the time lapse

between two consecutive scans is around 6s, the vertical displacements are not available in these intermediary periods.

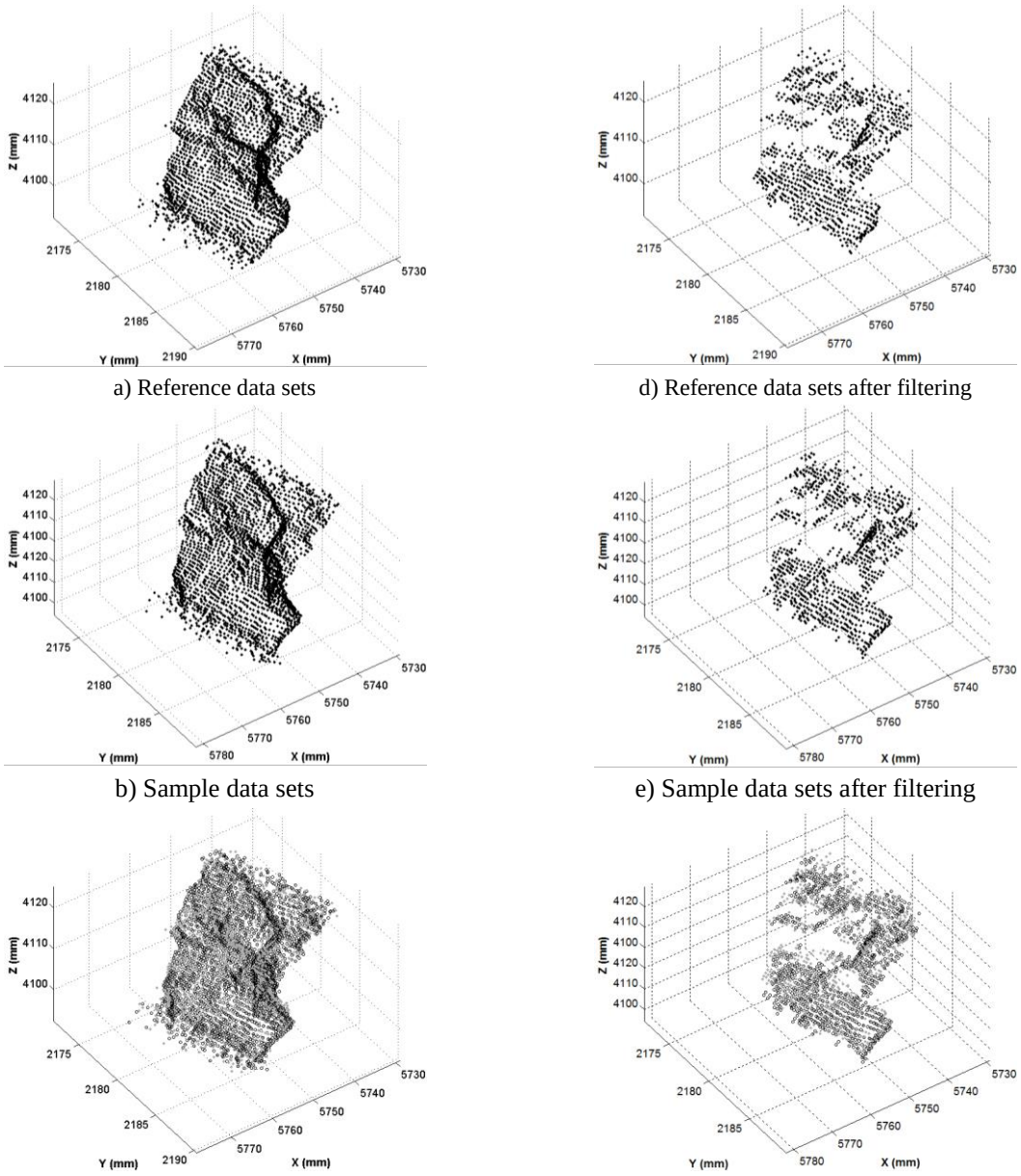

a) Reference data sets

d) Reference data sets after filtering

b) Sample data sets

e) Sample data sets after filtering

c) Overlaying two data sets

f) Overlaying two data sets after filtering

Fig. 5. Original and filtering reference and sample data sets

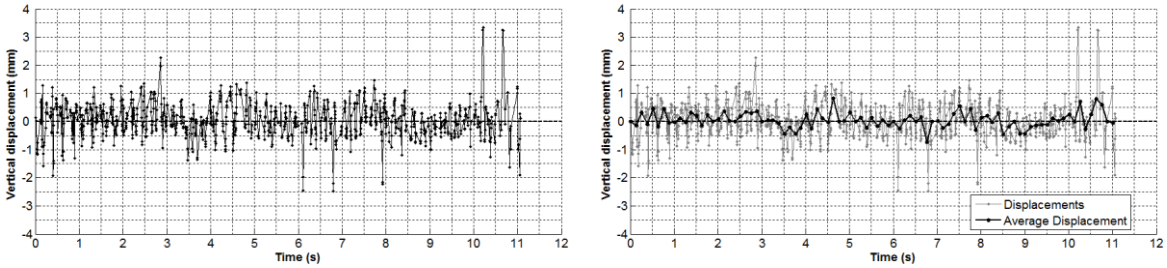

a) Displacements

b) Smoothing displacements with a time step by 0.125s

Fig. 6. Displacements and average displacements of the bridge beam over one scanning duration

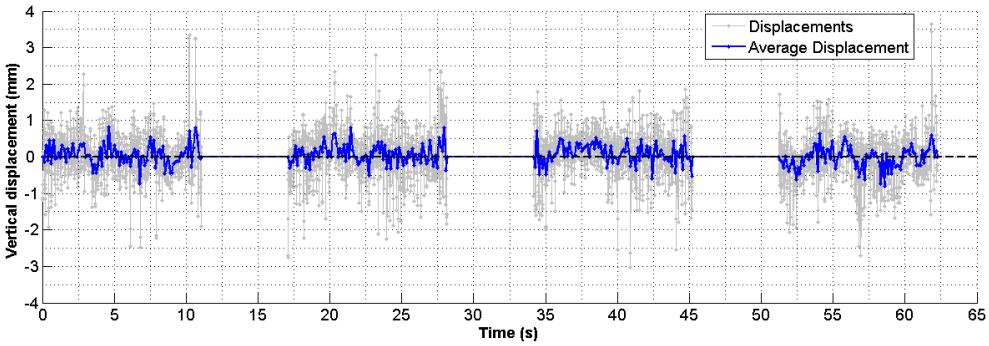

Fig. 7. Displacements and average displacements of the bridge beam from 4 consecutive scans

Discussion

Although TLS can acquire a point cloud for determining vertical displacements of a bridge without any other instrumentation (e.g. targets or scaffold) or traffic disruption, and reduce field time monitoring, applying TLS to dynamic bridge loading for deflection measurement still holds many challenges. Because the point cloud includes vertical surface of a steel plate and the bottom of the concrete beam extracting the data belonging to the horizontal planes is not trivial. Noise is another problem. With a small sampling step used, extensive surface details were scanned, but the highly noisy data appeared as an imperfectly smooth surface, and higher sampling steps may omit critical data. Thus, an appropriate sampling step should be investigated. Finally, a noise-filtering algorithm needs to be developed. Furthermore, no data can be captured during the time lapse between two consecutive scans. However, if these issues can be successfully overcome, TLS results could be used to compute a time history displacements, and the frequency of the structure can be then determined. As such, more useful information can be available in assessing bridge status than through other forms of bridge monitoring.

Conclusions

The current generation of commercial terrestrial laser scanners performs high speed collection of 3D data representing topographic object surfaces. The scanners offer the possibility of collecting sufficient data points to track object movements. This paper presents a preliminary study of using TLS in collecting vertical bridge movements due to dynamic vehicle loads. A point-surface based method is proposed for post-processing to calculate the bridge deflection. The Loughbrickland Bridge in Northern Ireland was selected as a case study, where the bridge deflection is measured over period. Results showed the vertical displacement directly derived from the point-surface based method varied in ±1mm while the smoothing displacement based a time interval was in a range of ±0.5mm. However, the accuracy level of the proposal method should be verified before implementing in practice. Furthermore, both an appropriate sampling step and a noisy filtering algorithm need to be investigated to minimize noise in the data set. The application of TLS in the point cloud acquisition for measuring time history displacement and deformation shape are ongoing research topics.

Acknowledgments

This work was support by the European Union's ERC-2012-StG_20111012 Project 307836. Dr. Tatsuya Ojio of the Department of Environmental Science and Technology, Meijo University in Japan organized access to the field site and assisted in data collection.

References

1. Casas J, Cruz, P. Fiber optic sensors for bridge monitoring. *Journal of Bridge Engineering 2003*, 8(6), 362-373.
2. Lee JJ, Shinozuka M. Real-time displacement measurement of a flexible bridge using digital image processing techniques. *Experimental Mechanics 2006*, 46(1), 105-114.
3. Yoneyama S, Kitagawa, A, Iwata, S, Tani, K, Kikuta, H. Bridge deflection measurement using digital image correlation. *Experimental Techniques 2007*, 31(1), 34-40.
4. Park HS, Lee, HM, Adeli H. A new approach for health monitoring of structures: Terrestrial laser scanning. *Computer-Aided Civil and Infrastructure Engineering 2007*, 22, 19-30.
5. González-Jorge H, Gonzalez-Aguilera, D, Rodriguez-Gonzalvez, P, Arias, P. Monitoring biological crusts in civil engineering structures using intensity data from terrestrial laser scanners. *Construction and Building Materials 2012*, 31, 119-128.
6. Laefer DF, Gannon J, Deely E. Reliability of crack detection for pre-construction condition assessments. *Journal of Infrastructure Systems 2010*, 6(2), 129-137.
7. Truong-Hong L, Laefer DF, Hinks T, Carr H. Flying voxel method with delaunay triangulation criterion for façade/feature detection for computation. *ASCE Journal of Computing in Civil Engineering 2012*, 26(6), 691–707.
8. Fuchs PA, Washer, GA, Chase, SB, Moore, M. Laser-based instrumentation for bridge load testing. *Journal of Performance of Constructed Facilities 2004*, 18(4), 213-220.
9. Riveiro B, González-Jorge H, Varela M, Jauregui DV. Validation of terrestrial laser scanning and photogrammetry techniques for the measurement of vertical underclearance and beam geometry in structural inspection of bridges. *Measurement 2013*, 46, 784-794.
10. Lichti DD, Gordon, SJ, Stawart, MP, Franke, J, Tsakiri, M. Comparison of digital photogrammetry and laser scanning. 2002.
11. Zogg H-M, Ingensand, H. Terrestrial laser scanning for deformation monitoring - load tests on the felsanau viaduct. *Proc., ISPRS Congress* 2008, 555-562.
12. Lovas T, Barsi, A, Detrekoi, A, Dunai, L, Csak, Z, Polgar, A, Berenyi, A, Kibedy, Z, Szocs, K. Terrestrial laser scanning in deformation measurements of structures. *Proc., ISPRS congress* 2008, 527-531.
13. Optech Incorporated. Field notes: Bridge deflection analysis. <http://www.optech.ca/pdf/Fieldnotes/ilris_bridge_deflection.pdf>, 2006. (07 January, 2014).
14. Kretschmer U, Abmayr T, Thies M, Frohlich C. Traffic construction analysis by use of terrestrial laser scanning. *Proc., IRPRS* 2002, 232-236.
15. Liu W, Chen, S, Hasuer, E. Bridge clearance evaluation based on terrestrial lidar scan. *Journal of Performance of Constructed Facilities 2012*, 26(4), 469-477.
16. Böhler W, Marbs, A. 3d scanning instruments. *Proc., Proceedings of the CIPA WG 6 International Workshop on Scanning for Cultural Heritage Recording* 2002, 9-18.
17. Blais F. Review of 20 years of range sensor development. *Journal of Electronic Imaging 2004*, 13(1), 231-240.
18. Lichti DD, Gordon, SJ. Error propagation in directly georeferenced terrestrial laser scanner point clouds for cultural heritage recording. *Proc., FIG Working Week 2004* 2004, 16.
19. Wehr A, Lohr, U. Airborne laser scanning-an introduction and overview. *ISPRS Journal of Photogrammetry & Remote Sensing 1999*, 54, 68-82.
20. Lichti DD, Sonam J. Angular resolution of terrestrial laser scanners. *The Photogrammetric Record 2006*, 21(114), 141-160.

21. Leica Geosystems. Leica scanstation p20. <http://www.leica-geosystems.com/downloads123/hds/hds/ScanStation_P20/brochures-datasheet/Leica_ScanStation_P20_DAT_en.pdf>, 2013. (5th April, 2014).
22. Trimble Navigation Limited. Trimble tx8 scanner. <http://trl.trimble.com/docushare/dsweb/Get/Document-687693/022516-014B_Trimble_TX8_DS_0114_LR.pdf>, 2013. (5th April, 2014).
23. Optech Incorporated. Ilris laser scanner. <http://www.optech.ca/pdf/Brochures/ILRIS-DS-LR.pdf>, 2009. (5th April, 2014).
24. RIEGL Laser Measurement Systems. Riegl vz-6000. <http://www.riegl.com/uploads/tx_pxpriegldownloads/DataSheet_VZ-6000_24-09-2012.pdf>, 2011. (5th April, 2014).
25. MathWorks. Matlab function reference.2010.